Energetics of Pyruvate Phosphate Dikinase Catalysis†

Andrew Mehl, Yuan Xu, and Debra Dunaway-Mariano*

Department of Chemistry and Biochemistry, University of Maryland, College Park, Maryland 20742

Received August 16, 1993; Revised Manuscript Received November 18, 1993®

ABSTRACT: The present study was carried out to determine the energetics of *Clostridium symbiosum* pyruvate phosphate dikinase (PPDK) catalyzed interconversion of adenosine 5′-triphosphate (ATP), orthophosphate (P_i), and pyruvate (pyr) with adenosine 5′-monophosphate (AMP), inorganic pyrophosphate, and phosphoenolpyruvate (PEP) [E·ATP ⇌ E-PP·AMP ⇌ E-PP·AMP·P_i ⇌ E-P·AMP·PP_i ⇌ E-P·pyr ⇌ E·PEP where E-PP and E-P represent the pyrophosphoryl and phosphoryl enzyme intermediates]. Thermodynamic techniques were used along with steady-state and pre-steady-state kinetic techniques to determine the rate constants for the substrate/product binding and release steps and the rate constants for the forward and reverse chemical steps. These values were used along with estimates of the cellular concentrations of the substrates and products to construct the free energy profile for the enzymatic reaction under physiological conditions. The energy profile obtained with the Mg^{2+}/NH_4^+-activated enzyme revealed well-balanced transition states and well-balanced internal ground state energies (i.e., within 1 kcal/mol of each other). Examination of the energetics of the reaction steps leading from ATP to phosphohistidine formation in E-P suggested the use of intrinsic binding energy in the synthesis of a high energy P–N linkage. Comparison of the energy profiles of the Mg^{2+}/NH_4^+- vs Co^{2+}/NH_4^+-activated enzymes revealed cofactor selectivity at each of the phosphophoryl transfer steps.

Pyruvate phosphate dikinase (PPDK)[1] is found in certain microbes and plants, and it catalyzes the interconversion of ATP, P_i, and pyruvate with AMP, PP_i, and PEP [for reviews, see Wood et al. (1977) and Cooper and Kornberg (1973)]. While the equilibrium position of the reaction favors ATP formation ($K_{eq} \approx 1 \times 10^{-2}$ for reaction 1;

$$\text{ATP} + P_i + \text{pyruvate} \rightleftharpoons \text{AMP} + PP_i + \text{PEP} \quad (1)$$

Reeves et al., 1968), the reaction can be easily driven in the direction of PEP by coupling it to the hydrolysis of PP_i catalyzed by pyrophosphatase. Thus, PPDK can serve in either ATP or PEP synthesis depending on the needs of the host organism. In *Clostridium symbiosum* and *Entamoeba histolytica*, PPDK functions in glycolytic ATP synthesis replacing pyruvate kinase, whereas in *Propionibacter shermanii*, *Acetobacter xylinum*, and C_4 plants PPDK substitutes for pyruvate carboxylase and PEP carboxykinase in PEP formation (Wood et al., 1977). Although *C. symbiosum* and plant (maize) PPDK carry out opposing physiological functions, they share a high degree of structural homology (about 50% sequence identity) (Pocalyko et al., 1990) and common catalytic steps (Carroll et al., 1990).

The PPDK reaction, written in the PEP-forming direction, involves the transfer of the ATP γ-phosphoryl group to P_i and the β-phosphoryl group to pyruvate (Reeves et al., 1968). The phosphoryl transfers are mediated by an active site histidine (Spronk et al., 1976). The histidine displaces AMP from the β-phosphoryl of ATP forming a pyrophosphorylated enzyme intermediate. Two sequential phosphoryl transfers ensue, first from the pyrophosphoryl histidine residue to P_i and then from the resulting phosphorylhistidine residue to pyruvate.

The present study was carried out to determine the energy profile of the *C. symbiosum* PPDK-catalyzed reaction. Aside from determining the rate-limiting step(s) for this reaction, we hoped to discover to what degree this enzyme is able to balance the energies of its internal states (Albery & Knowles, 1976). Herein, we report the thermodynamic and kinetic constants describing the substrate/product binding steps and the chemical steps. These values were used, along with estimates of the cellular concentrations of the substrates and products, to construct the free energy profile for the enzymatic reaction under physiological conditions. The influence of the divalent metal ion cofactor on the energetics of catalysis was examined by measuring energy profiles for both the Co^{2+}-activated enzyme as well as the Mg^{2+}-activated enzyme.

MATERIALS AND METHODS

General

[^{14}C]ATP, [^{14}C]pyruvate, and [γ-^{32}P]ATP were purchased from either Amersham or ICN Radiochemicals. [^{14}C]ATP and [γ-^{32}P]ATP were purified on a 1-mL DEAE Sephadex column by using a linear gradient of NH_4HCO_3 (0.3–0.6 M, 100 mL total volume) as eluant. [^{32}P]P_i, [^{32}P]PP_i, and [α-^{32}P]-AMPPNP were purchased from NEN. [β-^{32}P]ATP and [^{32}P]-PEP were prepared as described by Carroll et al. (1989). AMPPNP was obtained from Boehringer Mannheim Biochemicals. The HPLC system consisted of a Beckman 110A pump with a Beckman 420 controller interfaced with a variable wavelength Hitachi spectrophotometer. PPDK (*C. symbiosum*) was purfied from *Escherichia coli* JM101 cells transformed with the PPDK encoding recombinant plasmid pACYC184D12 (Pacolyko, 1990) by using the purification procedure described in Wang et al. (1988). Enzyme concentration was determined from A^{280} measurements. The

† This work was supported by NIH Grant GM-36260.

* To whom correspondence should be addressed.

® Abstract published in *Advance ACS Abstracts,* January 15, 1994.

[1] Abbreviations: PPDK, pyruvate phosphate dikinase; E-PP, pyrophosphorylenzyme; E-P, phosphorylenzyme; ATP, adenosine 5′-triphosphate; AMP, adenosine 5′-monophosphate; PEP, phosphoenolpyruvate; PP_i, inorganic pyrophosphate; P_i, inorganic phosphate; NADH, dihydronicotinamide dinucleotide; Hepes, *N*-(2-hydroxyethyl)piperazine-*N*′-ethanesulfonic acid; EGTA, ethylene glycol bis(β-aminoethyl ether)-*N*,*N*′-tetraacetic acid; AMPPNP, adenyl imidodiphosphate; PNP, imidodiphosphate.

0006-2960/94/0433-1093$04.50/0

subunit mass of 90 000 Da was used to calculate enzyme active site concentration. The turnovers numbers for Mg^{2+}/NH_4^+ and Co^{2+}/NH_4^+ activated PPDK in the forward and reverse reaction directions were determined as previously described (Thrall et al., 1993).

Rapid Quench Experiments

All rapid quench experiments were performed at 25 °C using a rapid quench instrument from KinTek Instruments (the three-syringe model) equipped with a thermostatically controlled circulator. A typical experiment was carried out by mixing a 43-μL solution of 30 mM K^+Hepes (pH 7.0) containing enzyme and cofactors with an equal volume of a buffered solution containing substrate(s). The reactions were quenched after a specified period of time with 164 μL of 0.6 N HCl. Next, 100 μL of CCl_4 was added, and the resulting solution was vortexed vigorously to precipitate the protein. The resulting mixture was then centrifuged and the supernatant siphoned from the protein pellet.

The E-P and E-PP formed in the reaction were quantitated by first washing the enzyme pellet with buffer (30 mM K^+-Hepes, pH 7.0) and then dissolving the pellet in 10 N H_2SO_4 at 100 °C for 1 min and adding it to scintillation fluid for counting (later we found the wash step was unnecessary and instead used a Kimwip to carefully remove excess solution from the pellet before dissolving in H_2SO_4). The [^{32}P]P_i present in the supernatant fraction of the reaction solution was quantitated by using the ammonium molybdate P_i extraction assay (Walter & Cooper, 1965). The radiolabeled PP_i, ATP, PEP, and AMP were separated from the supernatant fraction by using HPLC [Becknam Ultrasphere C18 analytical column and an isocratic gradient of 25 mM K^+P_i, 2.5% triethylamine, and 5% methanol (adjusted to pH 6.5 with H_3PO_4)]. A flow rate of 1.0 mL/min was employed in each case except for the separation of PEP in which a flow rate of 0.4 mL/min was used for 5 min to elute PEP, followed by a flow rate of 1.5 mL/min to elute the nucleotides. The radioactive peaks were collected with a fraction collector (250-μL fractions) and analyzed by scintillation counting.

Preparation of Phosphorylenzyme

The phosphorylated enzyme intermediate (E-P) was prepared by reaction of PPDK with excess PEP in the presence of NADH and LDH (lactate dehydrogenase). The reduction of the pyruvate formed by the phosphorylation step served to drive the reaction to completion and allowed us to monitor the reaction at 340 nm. A typical reaction solution consisted of 144 μM PPDK active sites, 2 mM PEP, 5 mM $MgCl_2$, 20 mM NH_4Cl, 500 μM DTT, and 300 μM NADH. The reaction was initiated by adding 0.5 unit of LDH. The observed decrease in absorbance of the reaction solution at 340 nm corresponded to the reduction of 144 μM pyruvate and, hence, the production of 144 μM E-P. Purification of E-P was achieved by chromatographing the reaction mixture on a Sephadex G-75 column (1 × 30 cm) with 50 mM K^+Hepes (pH 7.0).

Equilibrium Dialysis Experiments

The binding of AMPPNP to PPDK was measured using equilibrium dialysis techniques. Custom-made conical equilibrium dialysis cells (type D) described by Cheng and Carlson (1983) were used with Spectra/por membranes (12–14 000 Dalton molecular mass cut-off and a diameter of 100 mm). A 50-μL solution containing PPDK, cofactors, and buffer (30 mM K^+Hepes, pH 7.0) was loaded on one side of the membrane, and 50 μL of the AMPPNP solution (spiked with [α-^{32}P]AMPPNP, ≈ 20 000 cpm with a specific activity of 60 Ci/mol) was loaded on the other side. The concentration of enzyme active sites was 40 μM, and the concentration (based on a total volume of 100 μL) of $MgCl_2$ or $CoCl_2$ was 2.5 mM; NH_4Cl was 10 mM, and the concentration of AMPPNP varied from 2 to 300 μM. In one experiment 5 mM P_i was also included in the dialysis mixture. The cells were equilibrated by rotating at 25 rpm for at least 3 h at room temperature after which time a 35-μL aliquot was removed from each chamber and assayed for radioactivity via scintillation counting. The amount of enzyme-bound AMPPNP was determined by subtracting the amount of AMPPNP measured in the compartment without enzyme from the amount of AMPPNP that was measured in the compartment with enzyme.

P_i binding to PPDK was measured with and without (400 μM) AMPPNP present in the dialysis mixture. The concentration of enzyme active sites was 40 μM, and the concentration (based on a total volume of 100 μL) of $MgCl_2$ was 2.5 mM; NH_4Cl was 10 mM, and the concentration of P_i (spiked with ≈ 30 000 cpm of [^{32}P]P_i with a specific activity of 1 Ci/mmol) was varied from 2.5 to 80 μM in one experiment and from 100 to 800 μM in another experiment.

The binding of AMP to the E-P form of the PPDK was also measured by equilibrium dialysis. The concentration of E-P was 30 μM, $MgCl_2$ 2.5 mM, and NH_4Cl 12 mM. The AMP concentration (spiked with [^{14}C]AMP, about 25 000 cpm with a specific activity of 600 mCi/mmol) was varied from 2 to 30 μM. The data were analyzed in the form of a Scatchard plot.

PEP ↔ Pyruvate Molecular Isotope Exchange Experiments

Exchange reactions were carried out at 25 °C in 100 mM K^+Hepes (pH 7.0) with a final volume of 500 μL. All reactions contained 100 mM K^+Hepes (pH 7.0), 2 mM $MgCl_2$, 8 mM NH_4Cl, 100 μM DTT, and 0.007 μM PPDK active sites or 100 mM K^+Hepes (pH 7.0), 1 mM $CoCl_2$, 4 mM NH_4Cl, 0.1 mM β-mercaptoethanol, and 0.056 μM PPDK active sites. The concentration of [^{14}C]pyruvate was varied from 6 to 40 μM, and the concentration of PEP was varied from 5 to 100 μM. The exchange reactions were initiated by addition of enzyme. At specified times (at which 10–30% exchange had occurred) 50-μL aliquots were removed and quenched with 3 μL of 1.5 N HCl mixed with cold pyruvate and PEP and then analyzed by HPLC. A Beckman Ultrasil ion exchange column and an isocratic gradient of 0.45 M KCl and 15 mM KH_2PO_4 (pH 2.8) was run with a flow rate of 1 mL/min. The chromatography was monitored at 240 nm. The fractions containing pyruvate and PEP were assayed for radioactivity by using liquid scintillation counting techniques. The exchange velocities were calculated using eq 1 and analyzed according to eq 2 (Segel, 1975).

$$V_{ex} = -\frac{[PEP][PYR]}{[PEP] + [PYR]} \frac{2.3}{t} (\log 1 - f) \quad (1)$$

$$\frac{V_{ex}}{V_{ex}^{max}} = \frac{[PEP][pyruvate]}{K_D^{PEP}[PEP] + K_D^{pyr} + [PEP][pyruvate]} \quad (2)$$

Determination of the Overall Equilibrium Constant for the PPDK Reaction

The overall solution equilibrium constant for the PPDK reaction was determined by allowing a 492-μL buffered (100 mM K^+Hepes, pH 7.0) solution of ATP (0.935 mM), P_i (1.02

mM), [^{14}C]pyruvate (0.405 mM; SA = 6.0 mCi/mmol), PPDK (0.054 mg/mL; SA = 18.0 units/mg), and the required cofactors ($CoCl_2$ or $MgCl_2$, 5 mM; NH_4Cl, 20 mM) to equilibrate for 1 h at 25 °C. To determine when equilibrium was attained, aliquots (50 μL) were removed at varying conversions and quenched with 1 μL of 3 N HCl and analyzed by HPLC for [^{14}C]pyruvate and [^{14}C]PEP (for details of the separation, see the description under the PEP ↔ pyruvate molecular isotope exchange).

Determination of Internal Equilibrium Constants

The K_{eq} for E·PEP ⇌ E-P·pyruvate was determined by measuring the time course for a single turnover (see rapid quench section) of 40 μM PPDK with 1 mM [^{32}P]PEP, 1 mM pyruvate, 10 mM NH_4Cl, 50 mM K$^+$Hepes (pH 7.0), and 25 mM $MgCl_2$ or $CoCl_2$. The radiolabeled E-P formed was quantitated as described under the rapid quench experiments.

The K_{eq} for the E·ATP ⇌ E-PP·AMP reaction was determined by measuring the amount of radiolabeled E-PP formed from reaction of 1 mM [γ-^{32}P]ATP with 40 μM PPDK in the presence of 10 mM NH_4Cl, 50 mM K$^+$Hepes (pH 7.0), and 2.5 mM $MgCl_2$ or $CoCl_2$. The radiolabeled E-PP formed was quantitated as described under the rapid quench experiments.

Determination of the K_m for PP_i and K_i for PNP

The K_m for Co(PP_i) with Co^{2+}/NH_4^+-activated PPDK was determined by measuring the initial velocity of the catalyzed reaction as a function of Co(PP_i) concentration. The reaction mixture contained 100 mM K$^+$Hepes (pH 7.0), 1.0 mM PEP, 300 μM AMP, 5 mM NH_4Cl, and 300 μM uncomplexed $CoCl_2$. The concentration of Co(PP_i) was varied from 10 to 100 μM.

PNP was tested as a competitive inhibitor vs PP_i by measuring the initial velocity of the Mg^{2+}/PPDK-catalyzed reaction as a function of Mg(PP_i) concentration in the absence and in the presence of Mg(PNP). The reaction mixture contained 100 mM K$^+$Hepes (pH 7.0), 1.0 mM PEP, 300 μM AMP, 5 mM NH_4Cl, and 300 μM uncomplexed $MgCl_2$. The Mg(PP_i) concentration was varied from 10 to 500 μM, and the concentrations of Mg(PNP) were 0 and 100 μM. The initial velocity was measured by using the coupled spectrophotometric assay described by Wang et al. (1988) and analyzed in the form of a Lineweaver–Burk plot.

Rapid Quench Experiments To Determine Substrate Binding Rate Constants (k_{on})

Determination of the PEP Binding Rate Constant. All solutions were buffered with 100 mM K$^+$Hepes (pH 7.0). A buffered solution (43 μL) containing PPDK, $MgCl_2$ or $CoCl_2$, and NH_4Cl was mixed (in the rapid quench instrument) with a buffered solution (43 μL) containing [^{32}P]PEP. The final concentrations after mixing were 18 or 36 μM PPDK active sites, 2.5 mM $MgCl_2$, 10 mM NH_4Cl, and 0.11 μM [^{32}P]PEP (SA = 0.12 mCi/mmol). After a specified reaction period (ms) the solution was quenched with 164 μL of 0.6 N HCl. One hundred microliters of CCl_4 was added to the resulting solution, which was then vortexed vigorously to precipitate the protein. After centrifugation, a 150-μL aliquot of the resulting supernatant was removed and adjusted to pH 7 with 6 N NaOH. A 20-μL aliquot of this solution containing [^{32}P]-PEP was analyzed for radioactivity by liquid scintillation counting. The protein pellet containing [^{32}P]E-P was dissolved in 300 μL of 8 N H_2SO_4 at 100 °C (1 min) and then analyzed for radioactivity by liquid scintillation counting.

Determination of the Pyruvate Binding Rate Constant. A solution (43 μL) of E-P, $MgCl_2$ or $CoCl_2$, NH_4Cl, and 100 mM K$^+$Hepes (pH 7.0) was mixed with a solution (43 μL) of [^{14}C]pyruvate in 100 mM K$^+$Hepes (pH 7.0) with a rapid quench instrument. The concentrations of reactants and cofactors after mixing were 80 or 160 μM E-P active sites, 2.5 mM $MgCl_2$, or 1.0 mM $CoCl_2$, 10 mM NH_4Cl, and 2.0 μM [^{14}C]pyruvate (SA = 32 mCi/mmol). Following the acid quench and protein pelleting, the reaction sample was analyzed for [^{14}C]pyruvate and [^{14}C]PEP by using HPLC and liquid scintillation counting techniques (see above).

Determination of the P_i Binding Rate Constant. A solution (43 μL) of PPDK, $MgCl_2$, or $CoCl_2$, and NH_4Cl in 100 mM K$^+$Hepes (pH 7.0) was mixed with a solution (43 μL) of [^{32}P]P_i and ATP in 100 mM K$^+$Hepes (pH 7.0) with a rapid quench instrument. The concentrations of the reactants and cofactors after mixing were 30 μM PPDK active sites, 6.3 mM $MgCl_2$, or $CoCl_2$, 25 mM NH_4Cl, 2.0 μM [^{32}P]P_i (SA = 30 mCi/mmol), and 3 mM ATP. A 50-μL aliquot of the quenched reaction solution (see above) was analyzed for [^{32}P]P_i and [^{32}P]PP_i by using the ammonium molybdate P_i extraction assay.

Determination of the PP_i Binding Rate Constant. A solution (43 μL) of E-P, $MgCl_2$ or $CoCl_2$, and NH_4Cl in 100 mM K$^+$Hepes (pH 7.0) was mixed with a solution (43 μL) of [^{32}P]PP_i and AMP in 100 mM K$^+$Hepes (pH 7.0) with a rapid quench instrument. The concentrations of the reactants and cofactors after mixing were 40 μM E-P active sites, 2.3 mM $MgCl_2$ or $CoCl_2$, 9.3 mM NH_4Cl, 5.0 μM [^{32}P]PP_i (SA = 1 Ci/mmol), and 140 μM AMP. A 50-μL aliquot of the quenched solution (see above) was analyzed for [^{32}P]P_i and [^{32}P]PP_i by using the ammonium molybdate P_i extraction assay.

Determination of the ATP Binding Rate Constant. The concentrations of reactants and cofactors after mixing (43 μL of buffered enzyme and cofactors with 43 μL of buffered substrate) were 5 μM [γ-^{32}P]ATP, 35 μM PPDK active sites, 10 mM NH_4Cl, 50 mM K$^+$Hepes, and 2.5 mM $MgCl_2$ or $CoCl_2$. The reaction was quenched and the protein precipitated as described above. The protein pellet containing [^{32}P]E-PP was dissolved in 300 μL of 8 N H_2SO_4 at 100 °C (1 min) and then analyzed for radioactivity by liquid scintillation counting.

Pulse–Chase Experiments

Pulse–chase experiments were carried out by mixing an 80-μL solution of PPDK, radiolabeled substrate, metal ions, and buffer (the pulse) in a rapid quench apparatus. After a specified number of milliseconds, a 164-μL solution containing cosubstrate and a large excess of unlabeled substrate in buffer (the chase) was mixed with the pulse solution. After 3 s the reaction was terminated by the addition of 30 μL of 3 M HCl. The protein was then precipitated by the addition of 100 μL of CCl_4 to the reaction solution followed by vigorous vortexing. After centrifugation, the pH of the resulting supernatant was adjusted to 7 with 8 M NaOH and analyzed for radiolabeled substrate. The pulse solution for the AMP trapping experiment contained 6 μM [^{14}C]AMP, 40 μM E-P active sites, 6.3 mM $CoCl_2$ or $MgCl_2$, 25 mM NH_4Cl, and 25 mM K$^+$Hepes (pH 7.0). The chase solution contained 1 mM AMP, 10–1000 μM PP_i, and 25 mM K$^+$Hepes (pH 7.0). The pulse solution for PP_i trapping contained 1.2 μM [^{32}P]PP_i (SA = 3 Ci/mmol), 42 μM E-P active sites, 6.3 mM $MgCl_2$, 20 mM NH_4Cl_2, and 25 mM K$^+$Hepes (pH 7.0). The chase contained 5 mM PP_i, 5 mM AMP, and 25 mM K$^+$Hepes (pH 7.0).

Scheme 1: Kinetic Mechanism of the PPDK-Catalyzed Reaction As Reported in Thrall et al. (1993)

$$E+ATP \rightleftharpoons E{\cdot}ATP \rightleftharpoons E\text{-}PP{\cdot}AMP \overset{P_i}{\rightleftharpoons} E\text{-}PP{\cdot}AMP{\cdot}P_i \rightleftharpoons E\text{-}P{\cdot}AMP{\cdot}PP_i \overset{PP_i}{\rightleftharpoons} E\text{-}P{\cdot}AMP \overset{AMP}{\rightleftharpoons} E\text{-}P \overset{pyruvate}{\rightleftharpoons} E\text{-}P{\cdot}pyruvate \rightleftharpoons E{\cdot}PEP \rightleftharpoons E+PEP$$

RESULTS

General Methodology

Determination of the free energy profile of PPDK catalysis involved determination of the rate constants for the forward and reverse directions of the three chemical steps and of the five binding steps of the reaction sequence represented in Scheme 1 (Thrall et al., 1993). The general approach was to measure the equilibrium constants for the substrate/product binding steps and for the interconversion between central complexes and, where possible, the rate constants for the binding steps. Next, single-turnover time courses for both directions of the ATP + P_i + pyruvate $\rightleftharpoons$ E-P + PP_i + AMP reaction were measured. Finally, using the kinetics simulation program KINSIM (Barshop et al., 1983), the kinetic model of Scheme 1, and the experimentally obtained thermodynamic and kinetic constants, curves were simulated to fit (by an iterative process) the single-turnover time course data. In general, we found that the simulations defined the rate constants within a factor of 2. The rate constants were cross checked by using them to simulate curves to single-turnover profiles measured for the partial reactions. Since significantly different levels of the E-PP·AMP intermediate had been observed to accumulate with the Mg^{2+}/NH_4^+- and Co^{2+}/NH_4-activated forms of the enzyme (Carroll et al., 1989; Thrall et al., 1993), data were collected for both enzyme forms so that a comparison of the two energy profiles could be made.

Determination of the Equilibrium Constants for Binding Steps

ATP Binding. The K_d for the E·ATP complex was estimated by measuring the binding of the inert ATP analog, AMPPNP. Equilibrium dialysis techniques (see Materials and Methods) were used in conjunction with [α-^{32}P]AMPPNP to obtain a K_d = 52 ± 7 μM (77 ± 1 μM, trial 2; 66 ± 1 μM, trial 3) for the Mg^{2+}/NH_4^+-activated enzyme in the absence of P_i and K_d = 84 ± 1 μM in the presence of saturating (5 mM) P_i. These values compare with the K_i = 200 μM for MgAMPPNP derived from initial velocity studies (Wang et al., 1988). Thus a $K_{binding}$ range = 0.02–0.005 μM^{-1} was assumed in the simulations (Table 1).

A K_d = 7 ± 1 μM was obtained for [α-^{32}P]AMPPNP binding to the Co^{2+}/NH_4^+-activated enzyme as determined from the equilibrium dialysis data.

P_i Binding. We were unable to observe significant binding of P_i to the free enzyme or to the E·AMPPNP complex by using [^{32}P]P_i in conjunction with equilibrium dialysis techniques. On the basis of the detection limit for observing the E·P_i complex under the experimental conditions used, we estimate a minimum value for the K_d of P_i to be ~800 μM. This estimate is consistent with the results from other experiments which indicate that P_i binds weakly. Specifically, the K_m for P_i is 800 μM (Milner et al., 1975), and the K_i for P_i as a product inhibitor vs AMP and PP_i is ~4 mM (Wang et al., 1988). Finally, from a study of the P_i dependence of the rate of PPDK-catalyzed positional isotope exchange in ^{18}O-labeled ATP, the amount of P_i required for half-maximal exchange velocity was determined to be 2 mM (Wang et al., 1988). Thus, a K_d range of 800–4000 μM was assumed for E·ATP·P_i complex (independent of activating metal ion).

AMP Binding. The equilibrium dialysis technique was also used to measure the binding of [^{14}C]AMP to the E-P form of the enzyme. Analysis of the binding data in the form of a Scatchard plot yielded a K_d = 34 ± 6 μM for the Mg^{2+}/NH_4^+-activated enzyme.

PP_i Binding. The binding constant for PP_i binding to E-P·AMP was estimated by measuring the inhibition constant (K_i) of the inert PP_i analog PNP. PNP was used as a dead end inhibitor vs PP_i in initial velocity studies as described under Materials and Methods. The k_i of PNP as a competitive inhibitor of the Mg^{2+}/NH_4^+-activated enzyme was determined to be 25 μM.

PEP and Pyruvate Binding. The PEP and pyruvate equilibrium isotope exchange data were measured as described under Materials and Methods. A double-reciprocal plot of the exchange velocity (V_{ex}) vs pyruvate concentration at different fixed concentrations of PEP gave, in accord to eq 2, a series of parallel lines (Figure 1, Supplementary Material). A K_d = 140 μM for the Mg^{2+}/NH_4^+ E·P·pyruvate complex was determined from the slope of the lines while a K_d = 50 μM for E·PEP was determined from the X-intercept of the replot of the Y-intercepts va 1/[PEP]. For the Co^{2+}/NH_4^+-activated enzyme these values are 30 and 5 μM, respectively.

Transient Kinetic Determination of k_{on} Values for Substrates

The k_{on} values for the substrates were determined by measuring the rate of the reaction of a given substrate under conditions where substrate binding is rate limiting. These conditions were set by reacting the substrate at a very low concentration relative to that of the enzyme in the presence of saturating levels of cosubstrate. To test whether the binding step is truly rate limiting in the reaction under study, the reaction rate was determined at two different enzyme concentrations. Because the enzyme is used in excess, the rate of substrate binding is governed by the pseudo-first-order rate constant defined by the product $k_{binding}$[E], where the $k_{binding}$ [$=(k_{on}k_{cat})/(k_{off} + k_{cat})$] is less than or equal to k_{on} depending on the relative values of k_{off} (for substrate release) and k_{cat} (for substrate turnover).

PEP Binding. The rate constant for PEP binding to Mg^{2+}/NH_4^+-activated PPDK was determined by measuring the time course for the reaction of 0.11 μM [^{32}P]PEP with 18 and 36 μM enzyme (Figure 2, Supplementary Material). The observed rate for this process was determined to be 20 s^{-1} using [E] = 36 μM and to be 12 s^{-1} using [E] = 18 μM. The average $k_{binding}$ = 0.6 μM^{-1} s^{-1} was calculated and used as a lower limit for the rate of PEP binding in fitting the reaction profiles with KINSIM.

An approximate value for the rate of dissociation of PEP from the Mg^{2+}/NH_4^+ E·PEP complex was calculated by using the K_d for PEP determined by molecular isotope exchange data (K_D^{PEP} = 50 μM). These data allow us to estimate the value of the PEP k_{off} as ≥30 s^{-1}.

The same experiment was carried out to measure the time course profile for the formation of [^{32}P]E-P from a single-turnover reaction of [^{32}P]PEP and Co^{2+}/NH_4^+-activated PPDK. The observed rate was 1.0 s^{-1} for the 18 μM PPDK reaction and 1.7 s^{-1} for the 36 μM PPDK reaction. The average $k_{binding}$ = 0.05 μM^{-1} s^{-1} was used as the lower limit for the PEP k_{on}. From K_d = 5 μM the minimum k_{off} = 0.3 s^{-1} was calculated.

Table 1: Estimated and KINSIM (Kinetic Simulations) Generated Rate Constants for the Mg^{2+}/NH_4^+-Activated PPDK[a]

step	reaction	k_+ estimated	k_+ KINSIM	k_- estimated	k_- KINSIM	K_{eq} estimated	K_{eq} KINSIM
1	E + ATP ↔ E·ATP	≥5	4	≥300	525	50–200	131
2	E·ATP ↔ EPP·AMP		220		1100	0.08	0.2
3	EPP·AMP + P_i ↔ EPP·AMP·P_i	≥0.03	0.04	≥100	230	1000–3000	575
4	EPP·AMP·P_i ↔ EP·AMP·PP_i		850		250		3.4
5	EP·AMP·PP_i ↔ EP·AMP + PP_i	≥8	100	≥0.3	2.1	30	48
6	EP·AMP ↔ EP + AMP	≥200	180	5	2.5	40	72
7	EP + PYR ↔ EP·PYR	≥0.6	1	≥80	75	14	75
8	EP·PYR ↔ E·PEP		260		300	1	0.87
9	E·PEP ↔ E + PEP	≥30	125	≥0.6	0.75	50	170
	full reaction: ATP + P_i + PYR ↔ AMP + PP_i + PEP (k_+ = 5 s^{-1}; k_- = 16 s^{-1}; K_{eq} = 0.003)						0.006

[a] The reaction sequence refers to the kinetic mechanism shown in Scheme 1. Values are given in μM^{-1} s^{-1} for substrate on rates and s^{-1} for substrate off rates. All catalytic steps are in units of s^{-1}. Equilibrium constants for substrate binding steps and product release steps are given in units of μM.

Pyruvate Binding. The rate constant for pyruvate binding to Mg^{2+}/NH_4^+-activated E-P was determined by measuring the single-turnover time course profile for the formation of [^{14}C]PEP from the reaction of [^{14}C]pyruvate (2.0 μM) with E-P (80 and 160 μM active sites) (Figure 3, Supplementary Material). The apparent first-order rate constants were determined to be 82 s^{-1} ([E-P] = 160 μM) and 47 s^{-1} ([E-P] = 80 μM). The average $k_{binding}$ = 0.6 μM^{-1} s^{-1} was used to obtain the lower limit of PEP binding and, in conjunction with $K_d^{pyruvate}$ = 140 μM, to estimate the rate of pyruvate dissociation as ≥84 s^{-1}.

The rate of pyruvate binding to Co^{2+}/NH^{4+}-activated EP was measured in an analogous manner. A rate constant = 3.4 s^{-1} was determined for [E-P] = 160 μM and 2.4 s^{-1} for [E-P] = 80 μM. The average $k_{binding}$ = 0.03 μM^{-1} s^{-1} was used to obtain the lower limit for the rate of PEP binding. Using K_d = 50 μM a minimum k_{off} is calculated as 1.5 s^{-1}.

P_i Binding. The apparent first-order rate constant for P_i binding to Mg^{2+}/NH_4^+-activated PPDK was determined from a single-turnover reaction of [^{32}P]P_i (2.0 μM) with Mg^{2+}/NH_4^+-activated PPDK (30 μM) in the presence of 3 mM ATP (Figure 4, Supplementary Material). The apparent first-order rate constant was determined to be 0.09 s^{-1}. Since only ~10% of E·ATP will exist as E-PP·AMP, the concentration of enzyme in this form at the outset of the reaction is ~3 μM. Accordingly, the $k_{binding}$ is determined as ≥0.03 μM^{-1} s^{-1}. This value was used to set the minimum value of $k_{on}^{P_i}$ and, in conjunction with the $K_d^{P_i}$ range of 800–4000 μM, to provde an estimate of the minimum value for the $k_{off}^{P_i}$ to range from 20 to 120.

The single-turnover time course profile for the reaction of [^{32}P]P_i with excess ATP and Co^{2+}/NH_4^+-activated PPDK was measured using the same concentrations of reactants and cofactors given above. The pseudo-first-order rate for the reaction was determined to be 0.06 s^{-1}. Assuming that ~40% of the E·ATP present at the outset of the reaction will be E-PP·AMP (~11 μM), the $k_{binding}$ is 0.006 s^{-1}. This value was used to set the minimum value of $k_{on}^{P_i}$ and, in conjunction with the $K_d^{P_i}$ range of 8000–4000 μM, to provide an estimate of the minimum value for $k_{off}^{P_i}$ to range from 5 to 24 s^{-1}.

PP_i Binding. The apparent first-order rate constant for [^{32}P]PP_i (5 μM) binding to E-P (40 μM) in the presence of AMP (140 μM) was determined to be 11 s^{-1} for the Mg^{2+}/NH_4^+-activated enzyme and 3 s^{-1} for the Co^{2+}/NH_4^+ activated enzyme (Figure 5, Supplementary Material). Thus, the minimum k_{on} is 0.3 and 0.08 μM^{-1} s^{-1}, respectively. Assuming a K_d = 25 μM, k_{off} values of ≥8 and ≥2 s^{-1} are calculated.

ATP Binding. The apparent first-order rate constant for [γ-^{32}P]ATP (5 μM) binding to PPDK (35 μM) was determined to be 180 s^{-1} for the Mg^{2+}/NH_4^+-activated enzyme and 160 s^{-1} for the Co^{2+}/NH_4-activated enzyme (Figure 6, Supplementary Material). The minimum k_{on} is thus ~5 μM^{-1} s^{-1}. Assuming a k_d of ~50 μM for MgATP the k_{off} is ≥250 s^{-1}, and assuming a k_d of ~10 μM for CoATP the k_{off} is ≥50 s^{-1}.

Pulse–Chase Kinetic Determination of k_{off} Values for Products

AMP Release. To obtain an independent estimate for the k_{off} of AMP from E-P·AMP, a modified version of the standard pulse–chase method (Rose, 1980) was applied. Accordingly, freshly prepared E-P (40 μM active sites) plus Mg^{2+} (6.3 mM) and NH_4^+ (25 mM) were mixed with [^{14}C]AMP (6 μM) in a rapid quench apparatus and, after a specified number of milliseconds, mixed with a solution containing excess unlabeled AMP (1 mM) and a saturating level of PP_i (5 mM). The solution was then quenched within a 3 s by acid. The amount of [^{14}C]AMP trapped on E-P with PP_i (i.e., the amount of AMP converted to ATP) was plotted as a function of the time the [^{14}C]AMP was allowed to equilibrate with the E-P before the addition of the unlabeled AMP and PP_i (Figure 7, Supplementary Material). Since the reaction was carried out under pseudo-first-order conditions (i.e., [E-P] ≫ [^{14}C]-AMP]), the plot reflects the time course for AMP binding to E-P. Accordingly, an estimate of $k_{binding}$ = 8 μM^{-1} s^{-1} was calculated and used to set the minimum value for k_{on}^{AMP}.

To establish the PP_i concentration required for half-maximal trapping of [^{14}C]AMP, E-P was preincubated with Mg^{2+}, NH_4^+, and [^{14}C]AMP for 500 ms before the addition of unlabeled AMP and PP_i. The concentration of PP_i required for half-maximal [^{14}C]AMP trapped ($k_t^{PP_i}$) was determined to be 450 μM. According to the partition analysis described by Rose (1980), one can estimate that the rate of AMP dissociation k_{off}^{AMP} lies between the limits

$$(k_{cat})\frac{K_t^{PP_i}}{K_m^{PP_i}} < k_{off}^{AMP} > k_{cat}\frac{K_t^{PP_i}}{K_m^{PP_i}}\frac{[\text{E-P·AMP*}]}{P_\alpha^*}$$

where $K_m^{PP_i}$ is the Michaelis constant for PP_i (80 μM; Milner et al., 1975) and $P_\alpha^*/[\text{E-P·AMP*}]$ is the fraction of AMP trapped at saturating PP_i concentration (0.67) with a k_{cat} = 16 s^{-1} (see Table 1). These data place the rate of AMP dissociation to lie within the range 90–130 s^{-1}. From the K_d = 40 μM for the E-P·AMP complex (determined from equilibrium dialysis experiments), an AMP binding rate constant of 2 μM^{-1} s^{-1} is calculated. By assuming a dissociation constant of 18 μM for E-P·AMP as determined from the amount of AMP trapped (4 μM E-P·AMP from 6 μM [^{14}C]-AMP and 40 μM PPDK), the binding rate constant is

calculated to be $\sim 5\ \mu M^{-1}\ s^{-1}$. These k_{on} values compare favorably to the $k_{binding}$ rate of $8\ \mu M^{-1}\ s^{-1}$ determined from the time course.

A similar analysis was carried for the Co^{2+}/NH_4^+-activated PPDK. The concentration of PP_i required for half-maximal [^{14}C]AMP trapped is 70 μM. Since the dissociation constant for E-P·AMP was not determined by equilibrium dialysis, the amount AMP trapped (2 μM E-P·AMP from 34 μM E-P and 4 μM [^{14}C]AMP) was used to calculate a $K_d = 32\ \mu M$. From the values $k_t^{PP_i} = 70\ \mu M$, $K_m^{PP_i} = 10\ \mu M$ (see Materials and Methods), $k_{cat} = 3\ s^{-1}$, and fraction AMP trapped = 0.5, the range for k_{off} for AMP was calculated to be 20–40 s^{-1}. Using $K_d = 32\ \mu M$, the rate of AMP binding to E-P is calculated to be $\sim 1\ \mu M^{-1}\ s^{-1}$.

PP_i Release. Attempts to trap PP_i on E-P with AMP were unsuccessful (see Materials and methods). This result agrees with the reported (Wang et al., 1988) ordered of binding of AMP to E-P followed by PP_i.

Internal Equilibrium Constants

The internal equilibrium constant for E·ATP ⇌ E-PP·AMP was determined for single-turnover time course profiles of the reaction of 1 mM [γ-^{32}P]ATP with 40 μM PPDK. On the basis of K_d for E·ATP = 50 μM for Mg^{2+}/NH_4^+ and = 7 μM for Co^{2+}/NH_4^+ and the knowledge that AMP does not readily dissociate from E-PP·AMP, we assume that ~100% of the enzyme was complexed with ATP or AMP under these conditions. For the Mg^{2+}/NH_4^+-activated PPDK, 3 μM E-PP·AMP was formed, $K_{eq} = 0.08$. For the Co^{2+}/NH_4^+-activated PPDK, 14 μM E-PP·AMP was formed, $K_{eq} = 0.5$.

The internal equilibrium constant for E-P·pyruvate ⇌ E·PEP was determined by measuring the ratio of E to E-P formed for 40 μM PPDK in the presence of saturating levels of [^{32}P]PEP and pyruvate (1 mM each) as described under Materials and Methods. The $t_{1/2}$ to reach equilibrium in the Mg^{2+} system is ~3 ms and in the Co^{2+} system ~150 ms. The concentration of E-P formed, however, was the same for both systems, 20 μM ($K_{eq} = 1$).

Overall Solution Equilibrium Constant

The equilibrium constant for the PPDK-catalyzed interconversion of ATP, P_i, and pyruvate with AMP, PP_i, and PEP was determined by using [^{14}C]pyruvate in the equilibration reaction and measuring the [^{14}C]pyruvate/[^{14}C]PEP ratio at equilibrium. Highly pure and carefully calibrated samples of ATP, P_i, and [^{14}C]pyruvate were used in the initial reaction mixture. When equilibrium was achieved, the final concentrations of the ATP, P_i, and pyruvate were calculated by subtracting the amount of [^{14}C]PEP produced from the initial concentrations of the substrate. The reaction (25 °C) contained a catalytic amount of PPDK, 5 mM $MgCl_2$, 20 mM NH_4Cl, 0.405 mM [^{14}C]pyruvate, 0.935 mM ATP, and 1.02 mM P_i in 100 mM K^+Hepes (pH 7.0). At equilibrium 0.093 mM [^{14}C]PEP was present. The K_{eq} for the reaction was calculated using eq 3 to be 0.003.

$$K_{eq}(obs) = \frac{[AMP][PP_i][PEP]}{[ATP][P_i][pyruvate]} \quad (3)$$

The same conditions were employed in the determination of the K_{eq} for the Co^{2+}/NH_4-activated PPDK-catalyzed reaction in which 5 mM $CoCl_2$ was substituted for 5 mM $MgCl_2$. The [^{14}C]PEP formed at equilibrium was 0.130 mM yielding a $K_{eq} = 0.01$. The K_{eq} values were used to constrain the product of the equilibrium constants in the KINSIM simulations.

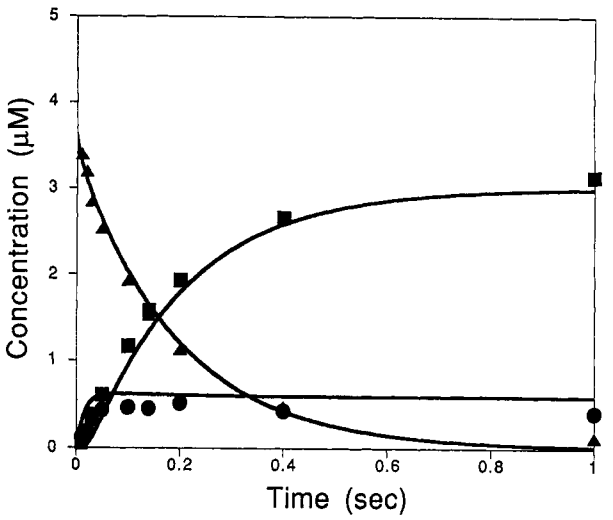

FIGURE 1: Time course for a single turnover of ATP, P_i, and pyruvate in the active site of Mg^{2+}/NH_4^+-activated PPDK at 25 °C. The reaction contained 3.6 μM [β-^{32}P]ATP, 32 μM PPDK active sites (subunit MW 90 000), 3 mM $MgCl_2$, 10 mM NH_4Cl, 8.5 mM P_i, 1 mM pyruvate, and 50 mM K^+Hepes (pH 7.0): (▲) ATP, (■) PEP, (●) E-PP + E-P.

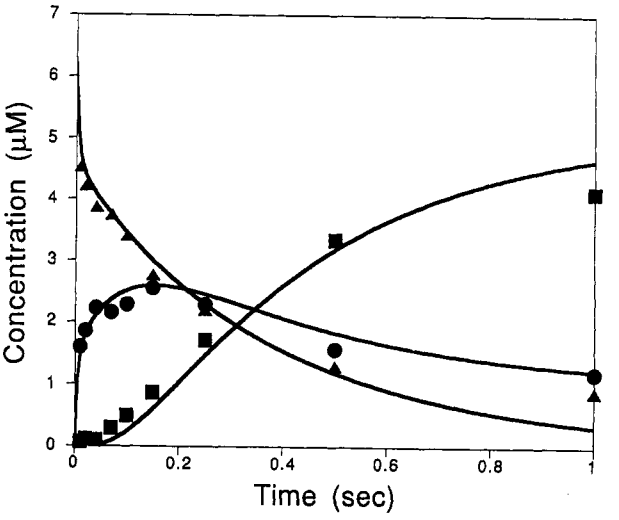

FIGURE 2: Time course for a single turnover of ATP, P_i, and pyruvate in the active site of Co^{2+}/NH_4^+-activated PPDK at 25 °C. The reaction mixture contained 6.2 μM [β-^{32}P]ATP, 40 μM PPDK active sites (subunit MW 90 000), 2.5 mM $CoCl_2$, 10 mM NH_4Cl, 2 mM P_i, 2 mM pyruvate, and 50 mM K^+Hepes (pH 7.0): (▲) ATP, (■) PEP, (●) E-PP + E-P.

Time Courses for Single Turnovers

The time courses for a single turnover in the PPDK active site were measured for the following reactions: E + [β-^{32}P]-ATP + P_i + pyruvate → AMP + PP_i + [^{32}P]PEP (profiles shown in Figure 1 for the Mg^{2+}/NH_4-activated enzyme and in Figure 2 for the Co^{2+}/NH_4^+-activated enzyme); E + [γ-^{32}P]-ATP + P_i + pyruvate → AMP + [^{32}P]PP_i + [^{32}P]PEP (profiles shown in Figure 3 for the Mg^{2+}/NH_4^+ activated enzyme and in Figure 4 for the Co^{2+}/NH_4^+-activated enzyme); and E + [^{32}P]PEP + AMP + PP_i → [β-^{32}P]ATP + P_i + pyruvate (profiles shown in Figure 5 for the Mg^{2+}/NH_4^+-activated enzyme and in Figure 6 for the Co^{2+}-activated enzyme).

The experimental values obtained for the binding constants (listed in Table 1 for the Mg^{2+}/NH_4^+-activated enzyme and Table 2 for the Co^{2+}/NH_4^+-activated enzyme) were used in conjunction with the kinetic model for the reaction pathway

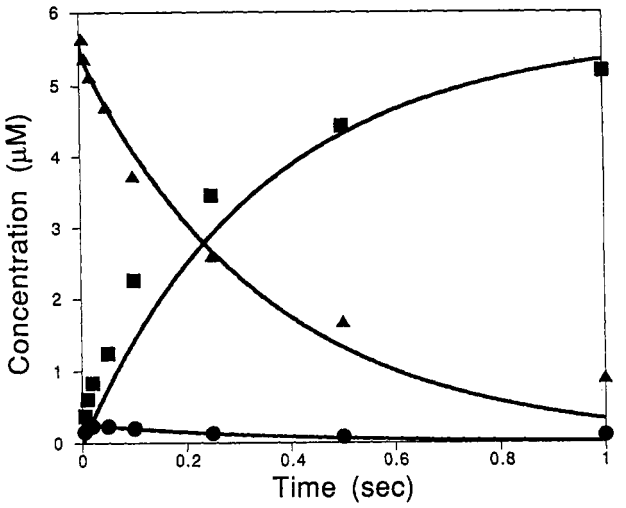

FIGURE 3: Time course for a single turnover of [γ-^{32}P]ATP in the active site of Mg^{2+}/NH_4^+-activated PPDK at 25 °C. The initial reaction mixture contained 5.7 μM [γ-^{32}P]ATP, 34 μM PPDK active sites (subunit MW 90,000), 1 mM pyruvate, 4 mM P_i, 2.5 mM $MgCl_2$, 10 mM NH_4Cl, and 50 mM K^+Hepes (pH 7.0): (▲) ATP, (■) PP_i, (●) E-PP.

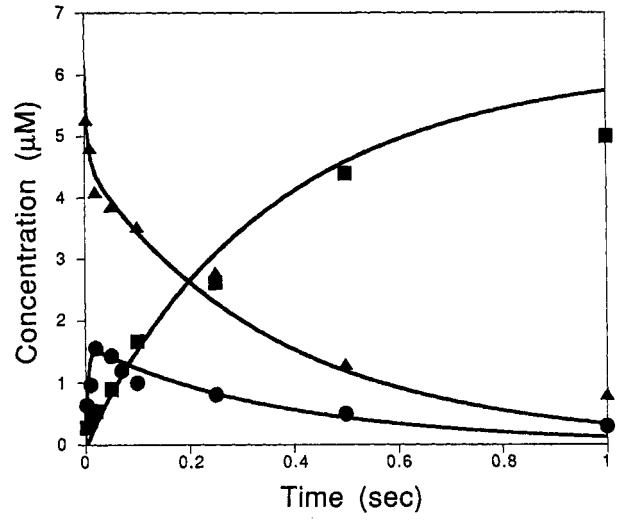

FIGURE 4: Time course for a single turnover of [γ-^{32}P]ATP in the active site of Co^{2+}/NH_4^+-activated PPDK at 25 °C. The initial reaction mixture contained 40 μM PPDK active sites (subunit MW 90 000), 50 mM K^+Hepes (pH 7.0), 2.5 mM $CoCl_2$, 10 mM NH_4Cl, 6.2 μM [γ-^{32}P]ATP, 2 mM P_i, and 2 mM pyruvate: (▲) ATP, (■) PP_i, (●) E-PP.

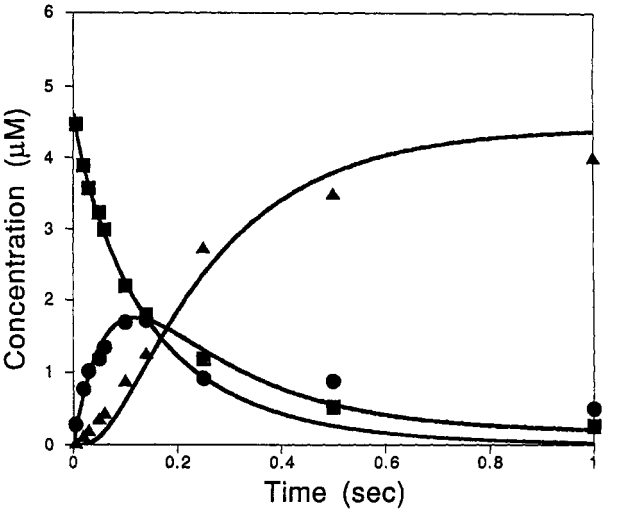

FIGURE 5: Time course for a single turnover of PEP, AMP, and PP_i in the active site of Mg^{2+}/NH_4^+-activated PPDK at 25 °C. The initial reaction mixture contained 4.6 μM [^{32}P]PEP, 32 μM PPDK active sites (subunit MW 90 000), 5 mM $MgCl_2$, 10 mM NH_4Cl, 20 μM AMP, 100 μM PP_i, and 50 mM K^+Hepes (pH 7.0): (▲) ATP, (■) PEP, (●) E-P + E-PP.

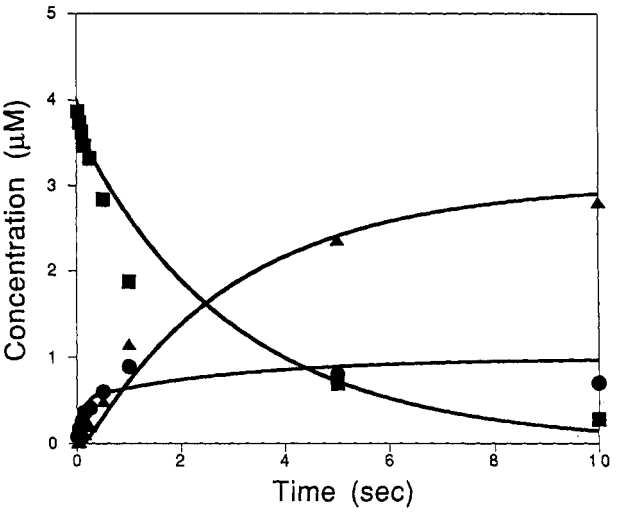

FIGURE 6: Time course for a single turnover of PEP, AMP, and PP_i in the active site of Co^{2+}/NH_4^+ activated PPDK at 25 °C. The initial reaction mixture contained 4.0 μM [^{32}P]PEP, 34 μM PPDK active sites (subunit MW 90 000), 2.5 mM $CoCl_2$, 10 mM NH_4Cl, 100 μM PP_i, 20 μM AMP and 50 mM K^+Hepes (pH 7.0): (▲) ATP, (■) PEP, (●) E-P + E-PP.

(Scheme 1) and the computer program KINSIM to simulate the time courses. Adjustments were made in the values of the rate constants until the simulated time courses closely matched the experimentally determined time courses. The rate constants used to generate the simulated curves were listed in Tables 1 and 2. Overall, the curves simulated using the kinetic model of Scheme 1 fit the experimental data quite well, and the rate constants used to arrive at the simulated curves are within reasonable agreement with those obtained experimentally (see Tables 1 and 2).

Free Energy Profiles for PPDK Catalysis

The rate constants derived through the simulation process (Tables 1 and 2) were used to construct energy profiles for PPDK catalysis. First, the energy profile for the partial reaction of E + ATP + P_i ⇌ E-P + AMP + P_i under the experimental conditions (5.9 μM ATP and 2 mM P_i) typically used to examine E-PP accumulation was determined for the Mg^{2+}/NH_4^+- and Co^{2+}/NH_4^+-activated PPDK. The ΔG^* values were calculated from the rate constants using the equation $\Delta G^* = RT[\ln(kB/Th) - \ln(k_{obs})]$, and ΔG values were calculated from the equilibrium constants using the equation $\Delta G = -RT \ln(K_{eq})$. The results are presented in Figure 7.

Next, the energy profile reflecting the energetics of the PPDK-catalyzed reactions *in vivo* was constructed. The rate and equilibrium constants for the binding and release steps were adjusted by using estimates of the concentrations of the substrates and products in the *C. symbiosum* cell as derived from their reported concentrations in *E. coli* (Kukko-Kalske & Heinonen, 1985; Lowery et al., 1971). The concentrations assumed are PEP, 0.08 mM; PP_i, 0.5 mM; AMP, 0.14 mM; pyruvate, 0.36 mM; P_i, 3.0 mM; and ATP, 2.4 mM. The profile of the Co^{2+}/NH_4^+-activated enzyme is compared to that of the Mg^{2+}/NH_4^+-activated enzyme in Figure 8.

Table 2: Estimated and KINSIM (Kinetic Simulations) Generated Rate Constants for the Co^{2+}/NH_4^+-Activated PPDK[a]

step	reaction	k_+ estimated	k_+ KINSIM	k_- estimated	k_- KINSIM	K_{eq} estimated	K_{eq} KINSIM
1	E + ATP ↔ E·ATP	5	5	50	35	10	7
2	E·ATP ↔ EPP·AMP		600		1500	0.5	0.40
3	EPP·AMP + P_i ↔ EPP·AMP·P_i	≥0.006	0.012	≥10	150	1000–3000	12500
4	EPP·AMP·P_i ↔ EP·AMP·PP_i		1000		300		4
5	EP·AMP·PP_i ↔ EP·AMP + PP_i	≥2	50	≥0.08	2	30	25
6	EP·AMP ↔ EP + AMP	30	60	1	3	30	20
7	EP + PYR ↔ EP·PYR	≥0.03	0.07	≥1.5	3	50	43
8	EP·PYR ↔ E·PEP		12		10	1	1.2
9	E·PEP ↔ E + PEP	≥0.3	20	≥0.05	0.15	5	130
	full reaction: ATP + P_i + PYR ↔ AMP + PP_i + PEP (k_+ = 2 s^{-1}; k_- = 3 s^{-1}; K_{eq} = 0.01)						0.033

[a] The reaction sequence refers to the kinetic mechanism shown in Scheme 1. Values are given in μM^{-1} s^{-1} for substrate on rates and s^{-1} for substrate off rates. All catalytic steps are in units of s^{-1}. Equilibrium constants for substrate binding steps and product release steps are given in units of μM.

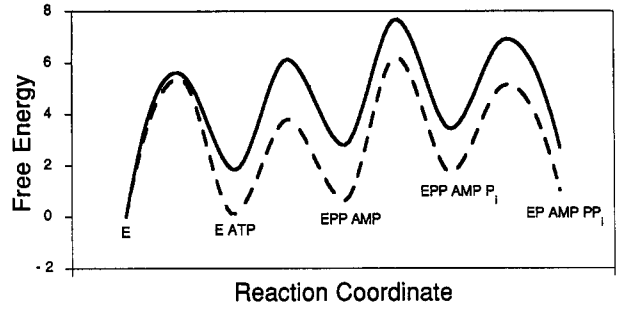

FIGURE 7: Reaction free energy profile for the Mg^{2+}/NH_4^+-activated PPDK (—) and for the Co^{2+}/NH_4^+-activated PPDK (- - -) showing the partial reaction of E + ATP + P_i ⇌ E-P·AMP·PP_i. The free energy change and the apparent free energies of activation for each step were calculated from the constants from Table 1 (Mg^{2+}) and from Table 2 (Co^{2+}). The concentrations of ATP and PP_i used in the calculations were 5.9 μM and 2 mM, respectively. 10 kcal/mol was subtracted from the energy of activation so that the relative heights of the transition states could be better depicted in this graph.

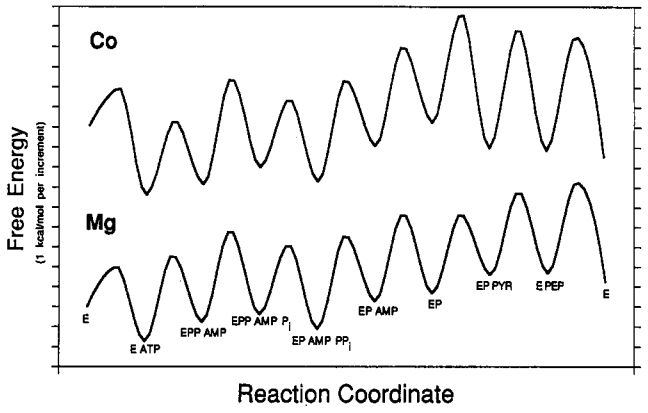

FIGURE 8: Reaction free energy profile for the Mg^{2+}/NH_4^+-activated PPDK and $Co/^{2+}/NH_4^+$-activated PPDK. The free energy change and the apparent free energies of activation for each step were calculated from the constants given in Tables 1 and 2. The concentrations of the substrates and products were set equal to the *in vivo* values determined for the bacterium *E. coli* as described in the text. 10 kcal/mol was subtracted from the energy of activation so that the relative heights of the transition states could be better depicted in this graph.

DISCUSSION

PPDK shares ancestry with *E. coli* PEP synthetase (Niersbach et al., 1992) and with enzyme I of the bacterial PEP: sugar phosphotransferase system (Pocalyko et al., 1990; Wu & Saier, 1990). PEP synthetase catalyzes the thermodynamically favorable (by ~2 kcal/mol) synthesis of PEP at the expense of both phosphodiester bonds in ATP (reaction 2) [for a review, see Cooper and Kornberg (1974)]. Like PPDK, PEP synthetase is believed to use an active site histidine to displace AMP from ATP to form a pyrophosphorylated enzyme intermediate (Narindarasorasak & Bridger, 1977). Phosphoryl transfer to H_2O (forming a phosphorylenzyme) and then to pyruvate follows. Enzyme I, on the other hand, is phosphorylated at the active site histidine with PEP and then catalyzes the phosphorylation of histidine of the HPr protein (reaction 3) [for reviews, see Postma and Lengeler (1985) and Saier (1989)].

$$\text{ATP} + H_2O + \text{pyruvate} \longrightarrow \text{AMP} + P_i + \text{PEP} \quad (2)$$

$$\text{EnzI-His} + \text{PEP} \xrightarrow{\text{pyruvate}} \text{EnzI-His-P} \xrightarrow{\text{HPr-His}} \text{HPr-His-P} \quad (3)$$

EnzI-His

Thus, PPDK, PEP synthetase, and enzyme I are linked not only by their structural homology but also through the use of a conserved active site histidine residue to mediate phosphoryl transfer. Previous studies have shown that the energy of this phosphohistidine in *C. symbiosum* PPDK (Milner et al., 1978) and *E. coli* enzyme I (Weigel et al., 1982) is quite high ($\Delta G°$ for hydrolysis ≈–14 kcal/mol), very close to that of the enol phosphate linkage in PEP ($\Delta G°$ for hydrolysis ≈–14.7 kcal/mol; Wood et al., 1966). These enzymes are well geared to catalyze phosphorylation of their active site histidine with PEP as well as phosphorylation of pyruvate with the phosphohistidine residue. The question which remains is how is the high energy phosphohistidine residue in PPDK and in PEP synthetase formed from ATP? (Copper & Kornberg, 1973; Wood et al., 1977; Frey, 1992). Specifically, while the sum of the energies of the two phosphoanhydride bonds in ATP (2 × 7.7 kcal/mol; Jencks, 1976) balances with that of the enzyme phosphohistidine linkage, the two phosphoanhydride bonds are cleaved in sequential steps generating a pyrophosphorylhistidine residue prior to forming the phosphohistidine residue. We wished to learn how, and to what extent, the energies of the complexes involving the apoenzyme, pyrophosphorylenzyme, and phosphorylenzyme are balanced.

Energy Profile of the Mg^{2+}/NH_4^+-Activated Enzyme. The rate constants for substrate binding to PPDK fall in the moderate range of 1–4 μM^{-1} s^{-1} with the exception of the P_i binding constant which is quite small (k_{on} = 0.04 μM^{-1} s^{-1}).[2] Slow P_i binding has also been observed with the enzyme EPSP synthase (P_i k_{on} = 0.07 μM^{-1} s^{-1}) (Anderson et al., 1988). The

high cellular concentration of P_i (3 mM in *E. coli*) apparently compensates for this small binding rate constant. The rate constants for the chemical steps of the PPDK reaction fall in the 2×10^2–1×10^3 s^{-1} range and, in general, exceed the k_{off} for product release by a factor of 2–3 (k_{off} values range from 100 to 500 s^{-1}).

The free energy profile (Figure 8) for the PPDK-catalyzed reaction under physiological conditions is characterized by well balanced (within ~1 kcal/mol) transition state energies and ground state energies. The highest energy transition state is associated with pyruvate binding; however, the energy margin is so small that it may be inaccurate to designate pyruvate binding as the rate-limiting step in the reaction.

Examination of the energetics of the reaction steps leading from ATP to phosphohistidine formation uncovers the strategy used by this enzyme for the synthesis of a high energy P–N linkage. Specifically, the energy difference between the α,β-phosphoanhydride bond in ATP and the phosphoamidate bond in E-PP ($\Delta\Delta G$ ~6 kcal/mol)[3] seems to be offset by the binding energy deriving from AMP and/or the pyrophosphorylhistidine residue. Exceptionally tight binding of AMP to the pyrophosphorylenzyme has been evidenced by molecular isotope exchange experiments which have shown that AMP is not in free exchange with the E-PP·AMP complex (Wang et al., 1988). In fact, the enzyme retains AMP until PP_i is formed and released.[4] In effect, the enzyme appears to be using differential binding of AMP to E-PP and E-P to supply pyruvate with a high energy phosphoryl donor.

Previous work on *C. symbiosum* PPDK by Wood and co-workers showed that the $\Delta G°$ for E-P hydrolysis is very closely matched with the $\Delta G°$ for PEP hydrolysis [–13.6 vs –14.7 kcal/mol (Milner et al., 1978; Wood et al., 1966)]. In the present study we found that the free enzyme binds PEP with the same affinity that E-P binds pyruvate and that the energies of the E·PEP and E-P·pyruvate complexes are balanced within a fraction of a kilocalorie. We do not know, based on present data, whether the pyruvate is bound to E-P in its keto or enol form. Rose and co-workers have shown that a substantial amount (20%) of the pyruvate bound in the pyruvate kinase active site is in the enol form (Seeholzer et al., 1991). Whether or not this is also the case for the pyruvate in the E-P·pyruvate complex remains to be tested.

Influence of the Metal Ion Cofactor on the PPDK Free Energy Profile. PPDK requires both a monovalent cation and divalent metal ion to serve as cofactors in catalysis (Michaelis et al., 1978; Moskovitz & Wood, 1978). The monovalent cation functions in the enolization of the pyruvate while the divalent metal ion is required in each of the phosphoryl transfer steps. Thus far only the E·PEP ⇌ E-P·pyruvate partial reaction has been studied with respect to the function of the divalent metal ion cofactor. Here it was found that the metal ion serves to coordinate both the pyruvate enol(ate) and the E-P phosphoryl group. *A priori* we expect that in the E + ATP + P_i ⇌ E-P + AMP + PP_i partial reaction the divalent metal ion activates ATP for phosphoryl transfer by chelate formation. Likewise, we anticipate activation of the pyrophosphoryl moiety of E-PP by direct metal coordination.

In earlier studies it was found that only Mg^{2+}, Co^{2+}, and Mn^{2+} function well in the divalent metal ion cofactor role (Michaels et al., 1978). The difference in the kinetic properties of these three metal ions as activators was exploited in recent single-turnover experiments to demonstrate the intermediacy of the pyrophosphorylenzyme in catalysis (Thrall et al., 1993). Specifically, reaction of excess PPDK with ATP leads to increasing amounts of E-PP·AMP when the metal cofactor was changed from Mg^{2+} to Co^{2+} and then to Mn^{2+} (from 4% conversion of ATP to E-PP·AMP for Mg^{2+} to 20% for Co^{2+} and 70% for Mn^{2+}). The Co^{2+} and Mn^{2+} enhancement of E-PP·AMP accumulation was also observed in the full reaction where E-PP·AMP serves as an intermediate (Carroll et al., 1989; Thrall et al., 1993). The overall V_{max} of the forward or reverse reaction catalyzed by for the Co^{2+}- or Mn^{2+}-activated enzyme is, however, significantly slower than that for the Mg^{2+}-activated enzyme (Michaels et al., 1978).[5]

To gain a better understanding of the impact of the divalent metal ion cofactor on the separate steps of catalysis, we determined the rate constants (Table 2) for catalysis by the Co^{2+}-activated enzyme for comparison to those obtained with the Mg^{2+}-activated enzyme (Table 1). The energy profile observed for the Co^{2+}/NH_4^+-activated enzyme shows less overall balancing of the energies of the ground state complexes and of the transition state complexes (Figure 8). The rates of both directions of the E·PEP ⇌ E-P·pyruvate catalytic step are adversely effected, which may account for the ~10-fold smaller V_{max} values (Tables 1 and 2) observed for the forward and reverse directions of the overall reaction. As noted previously, the divalent metal ion cofactor is believed to assist this catalytic step by bidentate coordination to the enol(ate) oxygen atom and carboxylate oxygen atom of the bound pyruvate and by monodentate coordinate to the phosphoryl group of the E-P. Why Mg^{2+} functions more effectively in this role than Co^{2+} has yet to be established.

Examination of the overlay of the free energy profiles (Figure 7) for the E + ATP + P_i ⇌ E-P + AMP + PP_i partial reaction calculated from substrate concentrations used in single-turnover experiments (rather than those representing physiological conditions) clearly illustrates why the observed E-PP levels (noted earlier) are higher with Co^{2+} serving as cofactor than with Mg^{2+}. First, equilibration of the Co^{2+}-activated enzyme and ATP leads to more E-PP·AMP as a result of both tighter ATP binding and greater E-PP·AMP stabilization. Second, in the presence of P_i, the Co^{2+} activated E-PP·AMP partitions forward slower than it is formed.

Conclusion. Measurement of the rate constants for the multistep catalysis by PPDK has allowed us to construct an energy profile for the physiological reaction which is consistent with a well evolved enzyme (Albery & Knowles, 1976) and has provided us with a glimpse of the multifaceted role played

[2] The k_{on} for ATP binding to PPDK (4 μM^{-1} s^{-1}) is closely matched with the k_{on} for ATP binding to glutamine synthetase (k_{on} = 2 μM^{-1} s^{-1}; Abel & Villafranca, 1991) while PEP binding to PPDK is considerably slower than PEP binding to EPSP synthase (k_{on} = 0.75 μM^{-1} s^{-1} vs k_{on} = 15 μM^{-1} s^{-1}; Anderson et al., 1988).

[3] This value is the difference between the reported $\Delta G°$ for hydrolysis of ATP at the α,β-position (–7.7 kcal/mol; Jencks, 1976) and the $\Delta G°$ for hydrolysis of the phosphohistidine residue in PPDK (–13.6 kcal/mol; Milner et al., 1978).

[4] Interestingly, Berman and Cohn (1970) concluded from their studies of the PEP synthetase reaction that AMP release must occur after the pyrophosphorylenzyme is converted to the phosphorylenzyme by reaction with H_2O.

[5] Michaels et al. (1978) had reported that Co^{2+} is an inferior activator in the PEP ⇌ pyruvate exchange reaction while Mn^{2+} is comparatively less active in the P_i ⇌ PP_i exchange reaction. Co^{2+}, Mn^{2+}, and Mg^{2+} were, however, reported to be equivalent in their ability to activate the ATP ⇌ AMP exchange reaction. Mehl (1991) found that the comparative ability of these metal ions to activate ATP ⇌ AMP exchange in the E + ATP + P_i ⇌ E-P + AMP + PP_i partial reaction varies sharply with reaction solution pH within the pH 6–8 region (the Co^{2+}-activated enzyme for example, was more active at pH 6 than 7 while the reverse was true for the Mg^{2+}-activated enzyme).

by the divalent metal ion cofactor. The dissection of PPDK catalysis into the individual steps will, in future studies, be used to study the mechanism of metal ion catalysis and to probe the role of enzyme active site residues in substrate binding and catalysis.

ACKNOWLEDGMENT

We thank Kenneth Johnson and Karen Anderson for many helpful discussions which took place during the course of this work.

SUPPLEMENTARY MATERIAL AVAILABLE

Seven figures giving time course data for the PPDK-catalyzed interconversion of ATP, P_i, and pyruvate with AMP, PP_i, and PEP (9 pages). Ordering information is given on any current masthead page.

REFERENCES

Abell, L. M., & Villafranca, J. J. (1991) *Biochemistry 30*, 6135.
Albery, W. J., & Knowles, J. R. (1976) *Biochemistry 15*, 5631.
Anderson, K. S., Sikorski, J. A., & Johnson, K. A. (1988) *Biochemistry 27*, 7395.
Barshop, B. A., Wrenn, R. F., & Frieden, C. (1983) *Anal. Biochem. 130*, 134.
Berman, K. M., & Cohn, M. (1978) *J. Biol. Chem. 245*, 5319.
Carroll, L. J., Mehl, A. F., & Dunaway-Mariano, D. (1989) *J. Am. Chem. Soc. 111*, 5965.
Carroll, L. J., Dunaway-Mariano, D., Smith, C. M., & Chollet, R. (1990) *FEBS Lett. 274*, 178.
Cheng, A., & Carlson, G. M. (1983) *Anal. Biochem. 10*, 370.
Cooper, R. A., & Kornberg, H. L. (1974) *The Enzymes* (Boyer, P. D., Ed.) Vol. X, 3rd ed., p 63, Academic Press, New York.
Frey, P. A. (1992) *The Enzymes* (Sigman, D. S., Ed.) Vol. XX, p 141–183, Academic Press, New York.
Jencks, W. P. (1976) in *Handbook of Biochemistry and Molecular Biology (3rd ed.) Physical and Chemical Data* (Fasman, G. D., Ed.) Vol. I, pp 296–304, CRC Press, Cleveland, OH.
Kukko-Kalske, E., & Heinonen, J. (1985) *Int. J. Biochem. 17*, 575.
Lowery, O. H., Carter, J., Ward, J. B., & Glaser, L. (1971) *J. Biol. Chem. 246*, 6511.
Mehl, A. F. (1991) Ph.D. Dissertation, University of Maryland, College Park, MD.
Michaels, G., Milner, Y., Moskovitz, B. R., & Wood, H. G. (1978) *J. Biol. Chem. 253*, 7656.
Milner, Y., Michaels, G., & Wood, H. G. (1975) *Methods Enzymol. 42*, 199.
Milner, Y., Michaels, G., & Wood, H. G. (1978) *J. Biol. Chem. 253*, 878.
Moskovitz, B. R., & Wood, H. G. (1978) *J. Biol. Chem. 253*, 884.
Narindrasorasak, S., & Bridger, W. A. (1977) *J. Biol. Chem. 252*, 3121.
Niersbach, M., Kreuzaler, F., Geerse, R. H., Postma, P. W., Hirsch, H. J. (1992) *Mol. Gen. Genet. 231*, 332.
Pocalyko, D. J. (1990) Ph.D. Thesis, University of Maryland, College Park, MD.
Pocalyko, D. J., Carroll, L. J., Martin, B. M., Babbitt, P. C., & Dunaway-Mariano, D. (1990) *Biochemistry 29*, 10757.
Postma, P. W., & Lengeler, J. W. (1985) *Microbiol. Rev. 49*, 232.
Reeves, R. E., Menzies, R. A., & Hsu, D. S. (1968) *J. Biol. Chem. 243*, 5486.
Rose, I. A. (1980) *Methods Enzymol. 64*, 47.
Saier, M. H. (1989) *Microbiol. Rev. 53*, 109.
Seeholzer, S. H., Jaworoski, A., & Rose, I. A. (1991) *Biochemistry 30*, 727.
Segel, I. H. (1975) *Enzyme Kinetics: Behavior and Analysis of Rapid Equilibrium and Steady State Enzyme Systems*, John Wiley and Sons, Inc., New York.
Spronk, A. M., Yoshida, H., & Wood, H. C. (1976) *Proc. Natl. Acad. Sci. U.S.A. 73*, 4415.
Thrall, S. H., Mehl, A. F., Carroll, L. J., & Dunaway-Mariano, D. (1993) *Biochemistry 32*, 1803.
Walter, E., & Cooper, C. (1965) *Anal. Biochem. 10*, 370.
Wang. H.-C., Ciskanik, L., vonder Saal, W., Villafranca, J. J., & Dunaway-Mariano, D. (1988) *Biochemistry 27*, 625.
Weigel, N., Kukuruzinska, M. A., Nakazawa, A., Waygood, E. B., & Roseman, S. (1928) *J. Biol. Chem. 257*, 14477.
Wood, H. G., Davis, J. J., & Lockmüller, H. (1966) *J. Biol. Chem. 241*, 5692.
Wood, H. G., O'Brien, W. E., & Michaels, G. (1977) *Adv. Enzymol. Relat. Areas Mol. Biol. 45*, 85.
Wu, L.-F., & Saier, M. H. (1990) *Mol. Microbiol. 4*, 1219.